

DEVELOPMENT OF HIGHLY-ACCURATE AND EXPLICIT INTERPOLATION POLYNOMIAL

By

Toshimitsu Komatsu

Koji Asai

Dept.of Civil Eng., Kyushu University, Fukuoka 812-81, Japan

and

Michihiro Mizunuma

West Japan Engineering Consultants. Inc., Fukuoka 810, Japan

SYNOPSIS

The six-point scheme proposed by Komatsu *et al.* for calculation of one-dimensional pure advection can be regarded as a highly-accurate interpolation cubic polynomial. An interpolation curve between two grid points can be obtained by applying the six-point scheme directly. However, the direct use of the six-point scheme does not always give the smooth curve because the continuity of the gradient of curve at grid points is not guaranteed. This paper presents a new interpolation cubic polynomial which is constructed on the basis of the six-point scheme and guarantees the continuity of the gradient. The accuracy of the new interpolation cubic polynomial is examined by using the time series data of three types of turbulence. It is found from the results that the new interpolation cubic polynomial has almost the same accuracy as the spline function and can be treated very easily because of its explicitness.

INTRODUCTION

The ungiven data between the data given discretely can be estimated by an interpolation. Scientists and engineers use an interpolation so often because most of data obtained by experiments or observations are not continuous but discrete. Representative interpolating functions used so far are the Lagrangian interpolation polynomial, the Newton's forward interpolating polynomial, the spline function and so on. The Lagrangian interpolation polynomial and the Newton's forward interpolating polynomial constitute a unique polynomial over the entire interpolation domain. As the number of used data increases, unnecessary oscillations generally become larger. On the contrary, the spline function gives a divided interpolation polynomial which seems to be best for each grid span and can give a smooth curve having little unnecessary oscillations. The spline function has a variety of applications, for example, numerical differentiation, numerical integration, computer aided design and so on. Therefore, the spline function is the most widely used interpolation and the powerful tool for science and engineering fields so far. However, it is necessary to solve the simultaneous equations the number of the unknown values of which is the same as that of the given data, so that the computational cost becomes more expensive as the number of the used data increases.

Komatsu *et al.* reported the six-point scheme(1) which was developed for calculation of one-dimensional pure advection. The six-point scheme is based on the characteristics method. As will be mentioned at the next section, the problem to estimate the value at a new time step at a spatial computational grid point can be reduced to the problem to obtain the value at an old time step at a spatial point

between two grid points. The value at the spatial point can be estimated by an interpolation. The six-point scheme is originally an interpolation cubic polynomial for a computational grid interval, which consists of the six known values. Therefore, the six-point scheme can be regarded as one of the highly-accurate interpolation cubic polynomials. Interpolating successive curves which pass through all given data points can be made by applying the six-point scheme to each grid interval. However, the interpolating curves obtained by the direct use of the six-point scheme in this way are not always smooth.

In this paper we have attempted to develop a new interpolation cubic polynomial which is based on the six-point scheme and able to provide the smooth curve easily. Test calculations have been carried out on the time series data of three types of turbulence in order to examine the accuracy of the new interpolation cubic polynomial. The results have shown that the new method has the excellent accuracy.

DERIVATION OF THE NEW INTERPOLATION CUBIC POLYNOMIAL

The Six-Point Scheme

The one-dimensional pure advection equation is written as

$$\frac{\partial \Phi}{\partial t} + u \frac{\partial \Phi}{\partial x} = 0 \quad (1)$$

where Φ =concentration of transported matter ; x =space coordinate ; t =time ; $u(x,t)$ =fluid velocity. Eq.(1) can be written as

$$\frac{d\Phi}{dt} = 0 \quad \text{along} \quad \frac{dx}{dt} = u \quad (2)$$

Eq.(2) implies that the fluid particle does not change its concentration while moving along the characteristic curve shown in Fig.1:

$$\Phi_i^{n+1} = \Phi_{\xi}^n \quad (3)$$

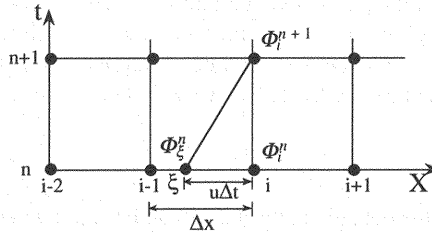


Fig.1 Computational grid

where superscript n denotes time level t_n ; subscript i denotes computational spatial point x_i ; ξ denotes the x -coordinate of the foot of the characteristics leading to the point (x_i, t_{n+1}) . Φ_{ξ}^n has to be estimated by an interpolation because the foot of the characteristics is not usually consistent with the computational grid point. The six-point scheme constitutes the highly-accurate interpolation cubic polynomial on interval $x_{i-1} \sim x_i$ using six known values around ξ in order to get the value of Φ_{ξ}^n . The details are described in the paper (1). The final expression of the six-point scheme is as follows:

$$\Phi_{\xi}^n = b_1 \alpha^3 + b_2 \alpha^2 + b_3 \alpha + \Phi_i^n \quad (4)$$

where

$$b_1 = a_{11} \Phi_{i-3}^n + a_{12} \Phi_{i-2}^n + a_{13} \Phi_{i-1}^n + a_{14} \Phi_i^n + a_{15} \Phi_{i+1}^n + a_{16} \Phi_{i+2}^n$$

$$b_2 = a_{21} \Phi_{i-3}^n + a_{22} \Phi_{i-2}^n + a_{23} \Phi_{i-1}^n + a_{24} \Phi_i^n + a_{25} \Phi_{i+1}^n + a_{26} \Phi_{i+2}^n$$

$$b_3 = a_{31} \Phi_{i-3}^n + a_{32} \Phi_{i-2}^n + a_{33} \Phi_{i-1}^n + a_{34} \Phi_i^n + a_{35} \Phi_{i+1}^n + a_{36} \Phi_{i+2}^n$$

$$a_{11} = -\frac{13}{720}; a_{21} = -\frac{3877}{101280}; a_{31} = \frac{17117}{303840};$$

$$a_{12} = \frac{37}{144}; a_{22} = \frac{1069}{20256}; a_{32} = -\frac{18821}{60768};$$

$$\begin{aligned}
a_{13} &= -\frac{49}{72} ; a_{23} = \frac{6563}{10128} ; a_{33} = \frac{31373}{30384} ; \\
a_{14} &= \frac{49}{72} ; a_{24} = -\frac{4705}{3376} ; a_{34} = -\frac{8717}{30384} ; \\
a_{15} &= -\frac{37}{144} ; a_{25} = \frac{5561}{6752} ; a_{35} = -\frac{34435}{60768} ; \\
a_{16} &= \frac{13}{720} ; a_{26} = -\frac{3121}{33760} ; a_{36} = \frac{22603}{303840}
\end{aligned}$$

in which α is a non-dimensional parameter which is the Courant number defined as $\alpha \equiv u\Delta t/\Delta x$ and can be regarded as an interpolating parameter. Eq.(4) is the cubic polynomial with respect to α and defined in the α -coordinate of which the positive direction is in consistency with the negative direction of x as shown in Fig.2.

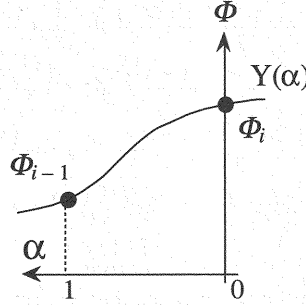


Fig.2 local coordinate of α

Derivation of INDUS

We shall consider a problem to make a new interpolation polynomial in this section. Therefore, the rest of this paper is not concerned with the pure advection problem. As mentioned above, Eq.(4) can be regarded as the highly-accurate interpolation cubic polynomial on interval $x_{i-1} \sim x_i$. By applying Eq.(4) to each data interval, divided interpolation polynomials can be obtained. However, the divided interpolation polynomials do not always give a smooth curve which is a continuous line of both value and gradient. To overcome this weakness Eq.(4) is used not directly as the interpolation polynomial but for estimating a gradient at a data point. We attempt to constitute a new interpolation polynomial by using the values and the gradients at the data points.

Let ΦX_i be the gradient at x_i . ΦX_i can be obtained by differentiating Eq.(4) applied to region I or region II shown in Fig.3. Let us note that $(\Phi X)_I$ and $(\Phi X)_{II}$ stand for the gradient at x_i evaluated by applying Eq.(4) to region I and II, respectively. $(\Phi X)_I$ and $(\Phi X)_{II}$ are written as follows:

$$\begin{aligned}
(\Phi X)_I &= a_{31} \Phi_{i-3} + a_{32} \Phi_{i-2} + a_{33} \Phi_{i-1} + a_{34} \Phi_i + a_{35} \Phi_{i+1} + a_{36} \Phi_{i+2} \\
&= \frac{17117}{303840} \Phi_{i-3} - \frac{18821}{60768} \Phi_{i-2} + \frac{31373}{30384} \Phi_{i-1} - \frac{8717}{30384} \Phi_i \\
&\quad - \frac{34435}{60768} \Phi_{i+1} + \frac{22603}{303840} \Phi_{i+2} \quad (5)
\end{aligned}$$

$$\begin{aligned}
(\Phi X)_{II} &= (3a_{11} + 2a_{21} + a_{31}) \Phi_{i-2} + (3a_{12} + 2a_{22} + a_{32}) \Phi_{i-1} + (3a_{13} + 2a_{23} + a_{33}) \Phi_i \\
&\quad + (3a_{14} + 2a_{24} + a_{34}) \Phi_{i+1} + (3a_{15} + 2a_{25} + a_{35}) \Phi_{i+2} + (3a_{16} + 2a_{26} + a_{36}) \Phi_{i+3} \\
&= -\frac{22603}{303840} \Phi_{i-2} + \frac{34435}{60768} \Phi_{i-1} + \frac{8717}{30384} \Phi_i - \frac{31373}{30384} \Phi_{i+1} \\
&\quad + \frac{18821}{60768} \Phi_{i+2} - \frac{17117}{303840} \Phi_{i+3} \quad (6)
\end{aligned}$$

$(\Phi X)_I$ is not always equal to $(\Phi X)_{II}$. This is the reason why Eq.(4) is not directly used as the divided interpolation polynomial. It is expected that the average on $(\Phi X)_I$ and $(\Phi X)_{II}$ gives a better estimation of the gradient at x_i . ΦX_i is given below.

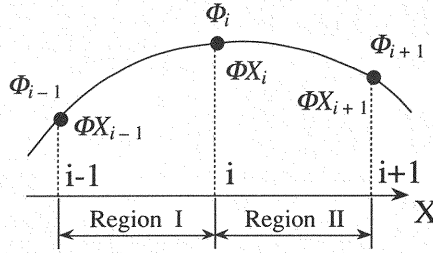


Fig.3 Definition of nodal gradient

$$\begin{aligned}
 \Phi X_i &= \frac{a_{31}}{2} \Phi_{i-3} + \frac{(3a_{11} + 2a_{21} + a_{31} + a_{32})}{2} \Phi_{i-2} + \frac{(3a_{12} + 2a_{22} + a_{32} + a_{33})}{2} \Phi_{i-1} \\
 &\quad + \frac{(3a_{13} + 2a_{23} + a_{33} + a_{34})}{2} \Phi_i + \frac{(3a_{14} + 2a_{24} + a_{34} + a_{35})}{2} \Phi_{i+1} \\
 &\quad + \frac{(3a_{15} + 2a_{25} + a_{35} + a_{36})}{2} \Phi_{i+2} + \frac{(3a_{16} + 2a_{26} + a_{36})}{2} \Phi_{i+3} \\
 &= \frac{17117}{607680} \Phi_{i-3} - \frac{29177}{151920} \Phi_{i-2} + \frac{97181}{121536} \Phi_{i-1} + 0 \Phi_i - \frac{97181}{121536} \Phi_{i+1} \\
 &\quad + \frac{29177}{151920} \Phi_{i+2} - \frac{17117}{607680} \Phi_{i+3} \quad (7)
 \end{aligned}$$

Let the order of interpolation polynomial be third and then we can make up a following cubic polynomial from four conditions, which are Φ_{i-1} , Φ_i , ΦX_{i-1} and ΦX_i .

$$Y_i(\alpha) \equiv P_i \alpha^3 + Q_i \alpha^2 + R_i \alpha + S_i \quad (8)$$

where

$$\begin{aligned}
 P_i &= \frac{17117}{607680} \Phi_{i-4} - \frac{33197}{202560} \Phi_{i-3} + \frac{369197}{607680} \Phi_{i-2} - \frac{145891}{121536} \Phi_{i-1} + \frac{145891}{121536} \Phi_i \\
 &\quad - \frac{369197}{607680} \Phi_{i+1} + \frac{33197}{202560} \Phi_{i+2} - \frac{17117}{607680} \Phi_{i+3}; \\
 Q_i &= -\frac{17117}{607680} \Phi_{i-4} + \frac{41237}{303840} \Phi_{i-3} - \frac{84163}{202560} \Phi_{i-2} + \frac{85123}{60768} \Phi_{i-1} - \frac{267427}{121536} \Phi_i \\
 &\quad + \frac{142517}{101280} \Phi_{i+1} - \frac{216299}{607680} \Phi_{i+2} + \frac{17117}{303840} \Phi_{i+3}; \\
 R_i &= \frac{17117}{607680} \Phi_{i-4} - \frac{29177}{151920} \Phi_{i-3} - \frac{84163}{202560} \Phi_{i-2} + \frac{85123}{60768} \Phi_{i-1} - \frac{267427}{121536} \Phi_i \\
 &\quad + \frac{142517}{101280} \Phi_{i+1} - \frac{216299}{607680} \Phi_{i+2} + \frac{17117}{303840} \Phi_{i+3}; \\
 S_i &= \Phi_i
 \end{aligned}$$

Introducing β ($\equiv 1 - \alpha = (x_i - x_{i-1}) / (x_i - x_{i-1})$) instead of α , we can obtain the final expression defined in the coordinate of which the positive direction is in consistency with the right hand direction.

$$\begin{aligned}
 Y_i(\beta) &\equiv -P_i \beta^3 + (3P_i + Q_i) \beta^2 + (-3P_i - 2Q_i - R_i) \beta + P_i + Q_i + R_i + S_i \\
 &= \left(-\frac{17117}{607680} \Phi_{i-4} + \frac{33197}{202560} \Phi_{i-3} - \frac{369197}{607680} \Phi_{i-2} + \frac{145891}{121536} \Phi_{i-1} - \frac{145891}{121536} \Phi_i \right. \\
 &\quad \left. + \frac{369197}{607680} \Phi_{i+1} - \frac{33197}{202560} \Phi_{i+2} + \frac{17117}{607680} \Phi_{i+3} \right) \beta^3 \\
 &\quad + \left(\frac{17117}{303840} \Phi_{i-4} - \frac{216299}{607680} \Phi_{i-3} + \frac{142517}{101280} \Phi_{i-2} - \frac{267427}{121536} \Phi_{i-1} + \frac{85123}{60768} \Phi_i \right. \\
 &\quad \left. - \frac{84163}{202560} \Phi_{i+1} + \frac{41237}{303840} \Phi_{i+2} - \frac{17117}{607680} \Phi_{i+3} \right) \beta^2 \\
 &\quad + \left(-\frac{17117}{607680} \Phi_{i-4} + \frac{29177}{151920} \Phi_{i-3} - \frac{97181}{121536} \Phi_{i-2} + 0 \Phi_{i-1} + \frac{97181}{121536} \Phi_i \right.
 \end{aligned}$$

Table 1 Mean turbulent energy and integral time scales of three types of turbulence

	$\overline{u'^2}$ (cm ² /sec ²)	T(sec)
Case-1(Oscillating-GridTurbulence)	83.19	1.43
Case-2(Turbulence of Open Channel Shear Flow)	0.64	4.16
Case-3(Turbulence on Internal Wave)	1.55	0.61

$$-\frac{29177}{151920} \Phi_{i+1} + \frac{17117}{607680} \Phi_{i+2} + 0 \Phi_{i+3} \Big) \beta + \Phi_{i-1} \quad (9)$$

Eq.(9) is the new divided interpolation polynomial proposed in this paper. Hereafter this method is labelled as INDUS (Interpolative Divided Polynomial Using Six-point scheme). Applying Eq.(9) to each data interval, we can easily obtain a smooth interpolation curve.

VERIFICATION OF THE ACCURACY OF INDUS

Interpolation of Time Series Data

When the data intervals are not small sufficiently compared with the variation scale of the data, a good interpolative data can not always be obtained. On discussing the accuracy of an interpolation, we should use the data involving the broad band of frequency of fluctuation. Therefore, the time series data of turbulent velocities are used to examine the accuracy of INDUS. The three types of data used here are the turbulence generated by an oscillating grid, the turbulence of open channel shear flow and the turbulence on internal wave. Table 1 shows the mean turbulent energy and the integral time scales of them. The result obtained by applying INDUS to Case-1 with the data interval Δt 1.0 sec is shown in Fig.4. The Newton's forward polynomial and the cubic B-spline function are adopted for comparison and the corresponding results are shown in Fig.5 and 6 respectively. Although interpolative curves do not follow the higher-frequency fluctuations than $f=1/2\Delta t$, we can find that INDUS has almost the same interpolative accuracy as the cubic B-spline function in these cases. The results for Case-2 with the data interval Δt 1.0 sec and for Case-3 with the data interval Δt 0.4 sec are shown in Figs.7~9 and Figs.10~12 respectively. As a result, it seems that INDUS has the same accuracy as the cubic B-spline function under the same conditions, whereas the Newton's forward polynomial has less accuracy than INDUS and/or the cubic B-spline function. The results shown in these figures suggest that the accuracy of the interpolation should be dependent on the ratio of the variation scale to the data interval. The comparison among these methods was made by using three kinds of turbulent data with the several data intervals. The results are shown in Figs.13~15. In these figures, the horizontal axis indicates the ratio of the data interval Δt to the integral time scale T, and the vertical axis indicates the normalized error that is the mean square of the difference between the experimental data and the interpolation divided by the turbulent intensity. u'

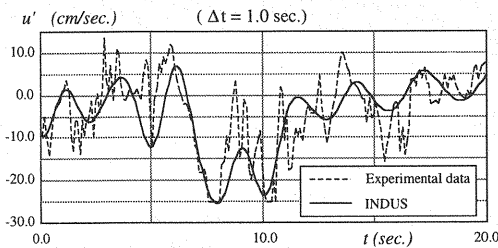


Fig.4 Result of interpolation for Case-1(INDUS)

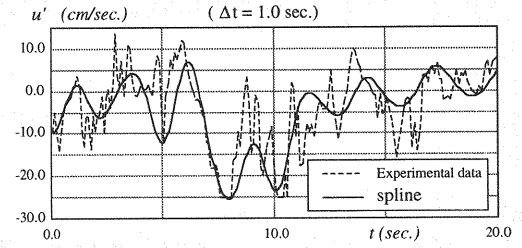


Fig.5 Result of interpolation for Case-1(Spline)

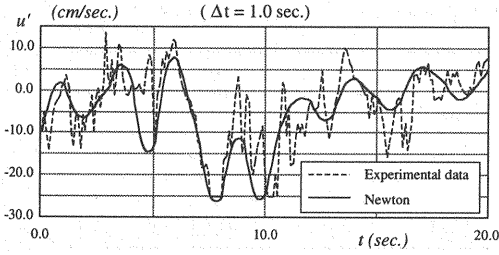


Fig.6 Result of interpolation for Case-1(Newton)

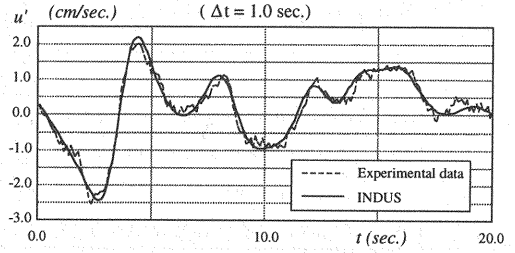


Fig.7 Result of interpolation for Case-2(INDUS)

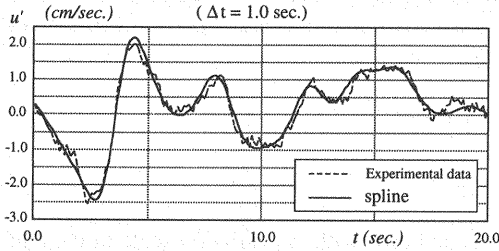


Fig.8 Result of interpolation for Case-2(Spline)

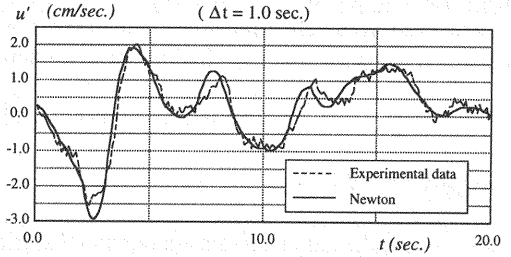


Fig.9 Result of interpolation for Case-2(Newton)

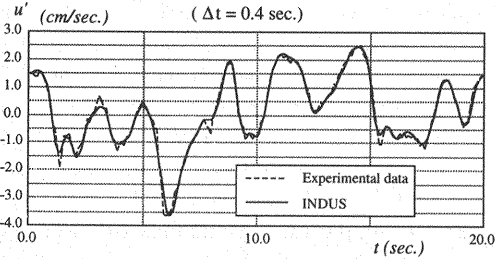


Fig.10 Result of interpolation for Case-3(INDUS)

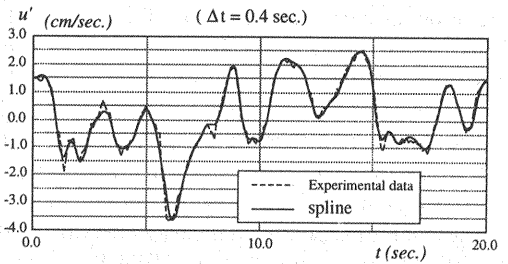


Fig.11 Result of interpolation for Case-3(Spline)

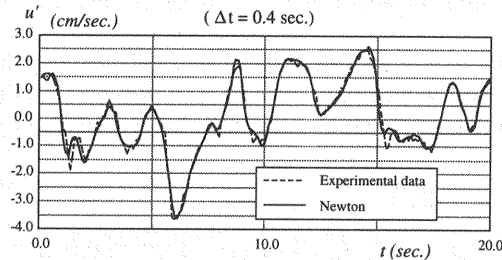


Fig.12 Result of interpolation for Case-3(Newton)

means the experimental data and u_i means the interpolation data. It can be seen from these figures that INDUS has almost the same accuracy as the cubic B-spline function for all data intervals and this characteristic is independent of the turbulent types used here. On the other hands, as the data interval ratio $\Delta t / T$ becomes larger the normalized error of Newton's forward polynomial tends to be large compared with the others methods.

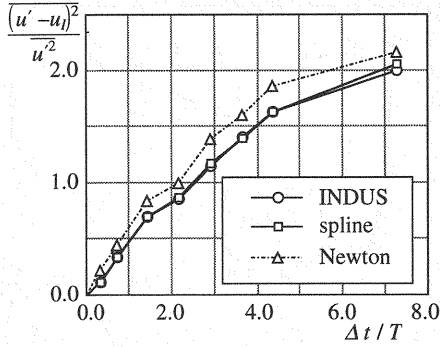


Fig.13 Comparison among the normalized errors associated with the three interpolation methods(Case-1)

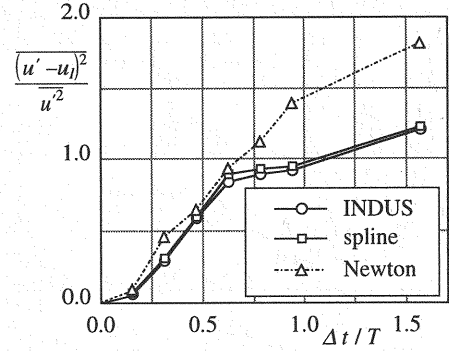


Fig.14 Comparison among the normalized errors associated with the three interpolation methods(Case-2)

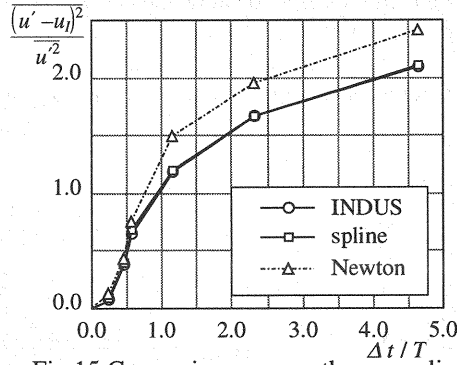


Fig.15 Comparison among the normalized errors associated with the three interpolation methods(Case-3)

Spectrum of Interpolation Data

INDUS does not work so well as an interpolation if the physical properties of turbulence change remarkably, even though the interpolation error seems to be small. Indeed, the use of interpolating cubic polynomial sometimes produces a large discrepancy in frequency properties. Therefore, the spectrum analysis was applied to the experimental data and the interpolation data. The spectra calculated for case-1 and case-2 are shown in Fig.16 and Fig.17 respectively. Theoretically speaking, the spectrum of the interpolation data can not reproduce the higher frequency components than $1/2\Delta t$. The obtained results show this tendency that the power is cut in the higher-frequency side. In addition, it can be recognized that the interpolation curve which is smoother than the experimental data tends to have the higher power amplified in the lower-frequency side.

The turbulent energy evaluated by integrating the power spectrum obtained from the spline function data over the whole frequencies is almost in agreement with that calculated from original experimental data, whereas that from INDUS was rather smaller than that from experimental data. This is due to the power-cut which is executed in higher-frequency side. It is apparent that INDUS has the excellent reproducibility in lower-frequency side.

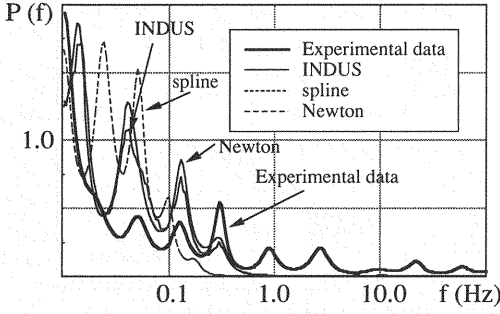


Fig.16 Power spectra of Case-1

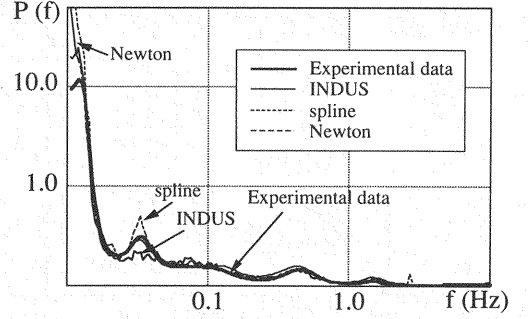


Fig.17 Power spectra of Case-2

APPLICATION OF INDUS TO BOUNDARY REGION

INDUS can be easily applied to a large number of data because of an explicit formulation. The application of INDUS to $i-1 \sim i$ region requires eight data, which are $\Phi_{i-4}, \Phi_{i-3}, \dots, \Phi_{i+2}$, and Φ_{i+3} . Therefore, INDUS is applicable to the regions from IV to N-3 shown in Fig.18, but needs some devices near the both boundaries if no data are given out of boundaries. This section deals with the modification of INDUS to make it applicable to the boundary region without out-boundary data.

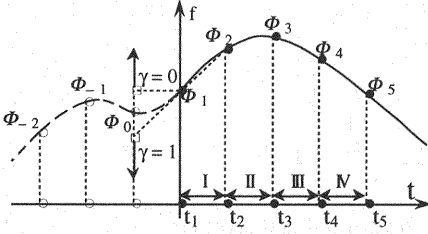


Fig.18-(a) Definition of the symbols in left-side boundary

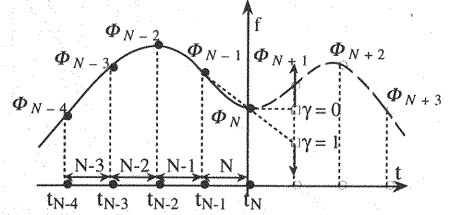


Fig.18-(b) Definition of the symbols in right-side boundary

Let us consider the left-side boundary. The value out of boundary, Φ_0 , shown in Fig.18-(a) is taken as follows:

$$\Phi_0 = (\gamma + 1) \Phi_1 - \gamma \Phi_2 \quad (10)$$

where γ is the weighting parameter. Eq.(10) takes a weighted average between the value estimated by a linear extrapolation when γ is equal to 1 and the value of Φ_1 when γ is equal to 0. The interpolation methods adaptable to the three regions near the boundary using Φ_0 and known data are shown below.

- (a) For region III: The interpolation polynomial is given by substituting Φ_0 and $\Phi_1 \sim \Phi_7$ into Eq. (9).
- (b) For region II: Φ_3' and Φ_2' denote the gradient at point t_3 estimated by differentiating the interpolation polynomial for region III and that at point t_2 obtained by substituting $\Phi_0 \sim \Phi_5$ into Eq.(6), respectively. The interpolation cubic polynomial for region II is constructed by using Φ_2, Φ_3, Φ_2' and Φ_3' .
- (c) For region I: The interpolation cubic polynomial can be given from four conditions which are Φ_1, Φ_2, Φ_2' obtained in the manner mentioned above and the gradient of a quadratic polynomial passing through the three data (Φ_0, Φ_1 and Φ_2) at point t_1 .

For the right-side boundary, the same manipulation as that for the left-side boundary will be implemented.

The interpolation calculations for the time series data of turbulence were carried out to decide the optimal value of γ . Fig.19 shows the relationship between γ and the normalized error, which has the same definition as before, but the average is made on only for the three region near the boundary. It is

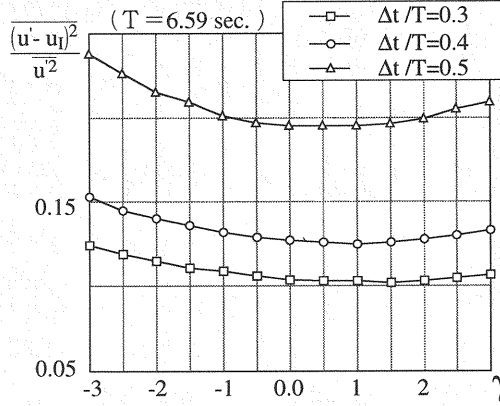


Fig.19 Relationship between γ and the normalized error

found from this figure that the accuracy of the interpolation is highest when γ is equal to 1. We should note that the parameter γ influences the results of the interpolations at the regions which are the closest to the boundaries, that is, the regions I and N. However, at the other regions the influence of γ is negligible. The interpolation polynomials for each region are formulated as follows:

$$\begin{aligned}
 Y_I = & \left(\frac{58957}{101280} \Phi_1 - \frac{45957}{33760} \Phi_2 + \frac{31373}{30384} \Phi_3 - \frac{18821}{60768} \Phi_4 + \frac{17117}{303840} \Phi_5 \right) \beta^3 \\
 & + \left(-\frac{58957}{101280} \Phi_1 + \frac{45957}{33760} \Phi_2 - \frac{31373}{30384} \Phi_3 + \frac{18821}{60768} \Phi_4 - \frac{17117}{303840} \Phi_5 \right) \beta^2 \\
 & + \left(\Phi_2 - \Phi_1 \right) \beta + \Phi_1
 \end{aligned} \quad (11)$$

$$\begin{aligned}
 Y_{II} = & \left(-\frac{21433}{75960} \Phi_1 + \frac{263513}{303840} \Phi_2 - \frac{29395}{30384} \Phi_3 + \frac{59539}{121536} \Phi_4 - \frac{41237}{303840} \Phi_5 + \frac{17117}{607680} \Phi_6 \right) \beta^3 \\
 & + \left(\frac{212701}{101280} \Phi_1 - \frac{22879}{15192} \Phi_2 + \frac{14203}{15192} \Phi_3 - \frac{2433}{13504} \Phi_4 + \frac{67}{844} \Phi_5 - \frac{17117}{607680} \Phi_6 \right) \beta^2 \\
 & + \left(-\frac{42323}{101280} \Phi_1 - \frac{12197}{33760} \Phi_2 + \frac{31373}{30384} \Phi_3 - \frac{18821}{60768} \Phi_4 + \frac{17117}{303840} \Phi_5 \right) \beta + \Phi_2
 \end{aligned} \quad (12)$$

$$\begin{aligned}
 Y_{III} = & \left(\frac{65357}{607680} \Phi_1 - \frac{489}{844} \Phi_2 + \frac{145891}{121536} \Phi_3 - \frac{145891}{121536} \Phi_4 + \frac{369197}{607680} \Phi_5 \right. \\
 & \quad \left. - \frac{33197}{202560} \Phi_6 + \frac{17117}{607680} \Phi_7 \right) \beta^3 \\
 & + \left(-\frac{49277}{202560} \Phi_1 + \frac{205217}{151920} \Phi_2 - \frac{267427}{121536} \Phi_3 + \frac{85123}{60768} \Phi_4 - \frac{84163}{202560} \Phi_5 \right. \\
 & \quad \left. + \frac{41237}{303840} \Phi_6 - \frac{17117}{607680} \Phi_7 \right) \beta^2 \\
 & + \left(\frac{41237}{303840} \Phi_1 - \frac{117197}{151920} \Phi_2 + 0 \Phi_3 + \frac{97181}{121536} \Phi_4 - \frac{29177}{151920} \Phi_5 + \frac{17117}{607680} \Phi_6 \right) \beta + \Phi_3
 \end{aligned} \quad (13)$$

$$\begin{aligned}
 Y_N = & \left(-\frac{17117}{303840} \Phi_{n-4} + \frac{18821}{60768} \Phi_{n-3} - \frac{31373}{30384} \Phi_{n-2} + \frac{45957}{33760} \Phi_{n-1} - \frac{58957}{101280} \Phi_n \right) \beta^3 \\
 & + \left(\frac{17117}{151920} \Phi_{n-4} - \frac{18821}{30384} \Phi_{n-3} + \frac{31373}{15192} \Phi_{n-2} - \frac{45957}{16880} \Phi_{n-1} + \frac{58957}{50640} \Phi_n \right) \beta^2
 \end{aligned}$$

$$+ \left(-\frac{17117}{303840} \Phi_{n-4} + \frac{18821}{60768} \Phi_{n-3} - \frac{31373}{30384} \Phi_{n-2} + \frac{12197}{33760} \Phi_{n-1} + \frac{42323}{101280} \Phi_n \right) \beta + \Phi_{n-1} \quad (14)$$

$$\begin{aligned} Y_{N-1} = & \left(-\frac{17117}{607680} \Phi_{n-5} + \frac{41237}{303840} \Phi_{n-4} - \frac{59539}{121536} \Phi_{n-3} + \frac{29395}{30384} \Phi_{n-2} \right. \\ & \left. - \frac{263513}{303840} \Phi_{n-1} + \frac{21433}{75960} \Phi_n \right) \beta^3 \\ & + \left(\frac{17117}{303840} \Phi_{n-5} - \frac{33197}{101280} \Phi_{n-4} + \frac{3265}{2532} \Phi_{n-3} - \frac{59779}{30384} \Phi_{n-2} \right. \\ & \left. + \frac{332959}{303840} \Phi_{n-1} - \frac{8899}{60768} \Phi_n \right) \beta^2 \\ & + \left(-\frac{17117}{607680} \Phi_{n-5} + \frac{29177}{151920} \Phi_{n-4} - \frac{97181}{121536} \Phi_{n-3} + 0 \Phi_{n-2} \right. \\ & \left. + \frac{117197}{151920} \Phi_{n-1} - \frac{41237}{303840} \Phi_n \right) \beta + \Phi_{n-2} \end{aligned} \quad (15)$$

$$\begin{aligned} Y_{N-2} = & \left(-\frac{17117}{607680} \Phi_{n-6} + \frac{33197}{202560} \Phi_{n-5} - \frac{369197}{607680} \Phi_{n-4} + \frac{145891}{121536} \Phi_{n-3} \right. \\ & \left. - \frac{145891}{121536} \Phi_{n-2} + \frac{489}{844} \Phi_{n-1} - \frac{65357}{607680} \Phi_n \right) \beta^3 \\ & + \left(\frac{17117}{303840} \Phi_{n-6} - \frac{216299}{607680} \Phi_{n-5} + \frac{142517}{101280} \Phi_{n-4} - \frac{267427}{121536} \Phi_{n-3} \right. \\ & \left. + \frac{85123}{60768} \Phi_{n-2} - \frac{58843}{151920} \Phi_{n-1} + \frac{67}{844} \Phi_n \right) \beta^2 \\ & + \left(-\frac{17117}{607680} \Phi_{n-6} + \frac{29177}{151920} \Phi_{n-5} - \frac{97181}{121536} \Phi_{n-4} + 0 \Phi_{n-3} + \frac{97181}{121536} \Phi_{n-2} \right. \\ & \left. - \frac{29177}{151920} \Phi_{n-1} + \frac{17117}{607680} \Phi_n \right) \beta + \Phi_{n-3} \end{aligned} \quad (16)$$

CONCLUSIONS

We developed a high-accurate explicit interpolative polynomial in this study. The results obtained in this paper are summarized as follows:

- (1) A new high-accurate explicit interpolative polynomial was developed and proposed based on the six-point scheme that is one of high-accurate schemes for calculating the pure advection equation.
- (2) INDUS has a great simplicity concerned with implementation because of its explicit expression. Therefore, it is easy to apply INDUS to the interpolation problem with a number of data.
- (3) The test problems and the spectrum analysis demonstrate that INDUS has comparable or higher accuracy than the cubic B-spline function.

REFERENCES

1. Komatsu, T., Holly, F.M., Nakashiki, N. and Ohgushi, K. : Numerical Calculation of Pollutant Transport in One and Two Dimensions, Journal of Hydrosience and Hydraulic Engineering, Vol. 3, No. 2, JSCE, pp.15-30, 1985.
2. Komatsu, T., Asai, and K., Mizunuma, M. : Development of Highly-Accurate and Explicit Interpolation Polynomial, Proceedings of the 37th Japanese Conference on Hydraulics, pp.751-756, 1993 (in Japanese).
3. Ed. Japan Society of Mechanical Engineers : Fundamentals of Computational Fluid Dynamics,

- CORONA Publishing CO.LTD., pp.14-18, 1988(in Japanese).
4. Ichita, K. and Yoshimoto, F. : Spline Function and Its Application, Educational Publishing CO.LTD., 1979 (in Japanese).
 5. Brice Carnahan, H.A. Luther and James O. Wilkes : Applied Numerical Methods, John Wiley & Sons, 1969.

APPENDIX – NOTATION

The following symbols defined below are used in this paper :

Φ	=	concentration of transported matter ;
Φ'	=	gradient of concentration ;
x	=	space coordinate ;
t	=	time coordinate ;
$u(x,t)$	=	fluid velocity ;
Δx	=	grid spacing ;
ξ	=	foot of the characteristics ;
$\alpha \equiv u \Delta t / \Delta x$	=	interpolating parameter ;
i	=	x-direction grid index point ;
n	=	t-direction grid index point ;
Φ_{Xi}	=	gradient of Φ at Xi ;
β	\equiv	$1 - \alpha = (x_{\xi} - x_{i,l}) / (x_i - x_{i,l})$;
$Y_i(\alpha)$	=	new interpolating polynomial in terms of α ;
$Y_i(\beta)$	=	new interpolating polynomial in terms of β ;
u'	=	velocity fluctuation ;
u^2	=	turbulent intensity ;
Δt	=	data interval ;
T	=	integral time scale ;
u_l	=	interpolation data ; and
γ	=	weighting parameter.

(Received November 30, 1994; revised April 24, 1995)